A Novel Experimental Approach to the Evaluation of Thermal Expansion Parameters of Solid Materials

A. F. ALTZOUMAILIS[1*], V. N. KYTOPOULOS[2]

[1*]School of Chemical Engineering, National Technical University of Athens,
5, Heroes of Polytechnion Avenue,
15773 Athens,
GREECE

[2]School of Applied Mathematical and Physical Sciences,
National Technical University of Athens,
5, Heroes of Polytechnion Avenue,
15773 Athens,
GREECE

Abstract: In this work a micromagnetic emission – aided experimental approach is presented by which the coefficients of thermal expansion (CTE) and related thermoelastic Young's as well as respective plastic moduli of various solids can optimally be evaluated. For this scope, certain well- established characteristics of stress (strain) – correlated ferromicromagnetic properties of Ni (nickel) material were used as basic- reference measuring parameters. In this context a well- determined Ni- based layer was produced by vapor deposition on the surface of tested substrate material. This layer in turn was utilized as a suitable sensor for its micromagnetic emission – response to stresses (strains) developed during simultaneous thermal cooling of Ni – layer and respective substrate. The substrate form of metallic oxides were prepared by suitable thermal oxidation treatment of the respective metal, where the desired quality and thickness of obtained oxide scale could be achieved with acceptable tolerance. As such, the reliability, versatility and conveniency of the proposed measuring technique was tested on the basis of titanium and nickel as well as three types of metallic oxides, i.e. MgO (magnesia) TiO_2 (rutile) and Mn_3O_4 (Hausmannite). This was possible by subjection of these materials to controlled thermal cooling procedure within given temperature ranges. In this way one can demonstrate that the obtained experimental data concerning the overall- average as well as instantaneous CTE of these materials are in reasonable agreement with those found in the related literature. It was also found that the order of magnitude of the evaluated thermoelastic and plastic moduli were also in reasonably agreement with data in the respective literature. It should, however, be mentioned that owing to the scarcity of detailed data on these parameters, a more systematic and reliable assessment of the obtained values could not be made.

Keywords: oxide, coefficient, thermal expansion, strain, stress, modulus, substrate, Ni- layer, temperature range.

Received: April 25, 2024. Revised: November 17, 2024. Accepted: December 9, 2024. Published: December 31, 2024.

1. Introduction

One of the crucial requirements for modern technological materials is their performance at elevated temperature. This may explain the increasing interest in studying the various temperature – induced changes in the thermomechanical properties of these materials. For example elastic modulus is a basic characteristic of the mechanical behavior of a given ideal (defect – free) and real (with defects) material. This modulus is closely

related to the atom structure and substantially affects a number of physical and technical properties of the material such as its thermal properties for instance its thermal expansion. Of a more direct importance nowadays are some engineering aspects of this modulus which is a vital consideration in high temperature structural design of stress and strain calculations. By the way, almost as important as the modulus E it is its variation with temperature expressed by the temperature coefficient of modulus of elasticity which in many applications must be suppressed as far as possible such as for audio-frequency calibration standards, electromagnetical filters etc. However, the data available for the respective situations should be regarded as only approximate because the literature contains widely different E- modulus value for one and the same material especially for alloys and composites. These discrepancies are apparently due to differences between experimental methods employed to establish the data. Consequently, the role of experimental techniques for the evaluation of elastic modulus under high temperature conditions becomes quite important. However, direct measurements of thermoelastic modulus at different temperatures is rather a difficult task, especially for advanced metallic oxides and non-oxide ceramics because of the relative complexity of high temperature measuring set-ups. Furthermore, metals and their oxides may undergo appreciable dimensional changes in response to large temperature changes, a physical phenomenon that may have detrimental implications for various manufacturing processes of these materials. Metallurgical operations such as rollying, extrusion, deep drawing etc. can significantly be influenced due to thermal stresses and associated strains that arise from such changes. Moreover, residual (permanent) stresses and mechanical distortions, caused by such operations may introduce various damages such as microcracking or even fracture of materials. In addition, most industrial applications of high melting materials may involve considerable temperature variations caused by in- service thermal cycling operations. In particular, complete cooling of a structural component to ambient temperature may occur very often in practice and the coefficients of thermal expansion of the related material are therefore probably to be of crutial importance in evaluating the respective residual stresses that are generated. It results, that an optimization of such operations requires quite comprehensive data on coefficient of thermal expansion (CTE) of the respective material. Thus the availability of such data at high temperatures becomes a very important issue. In this aspect a great variety of empirical or semi- empirical experimental techniques have been introduced for the measurement of CTE with particular paid to their conveniency, accuracy, and versatility. In these techniques the evaluation of CTE requires the measurement of displacement and temperature for the specimen subjected to the given – desired range of thermal changes. In this manner many different more or less sophisticated experimental approaches have been proposed some of which are absolute techniques while others relative ones that utilize standard- reference materials [1, 2]. Thus the great diversity of these techniques is reflected by the different methods applied to measure the related displacements. Thereafter, the problem of an optimum technique arises, fact which would involve a compromise between the existing gaps of high temperature processing, range of temperature change, accuracy of measurements and efforts of specimen preparation, Furthermore, due to the relative scarcity of available data on CTE there will be an urgent need for additional and more empirical measuring approaches to the above mentioned thermostatical properties by means of entirely novel techniques. As such, in the present work an attempt is made to develop and apply an empirical technique consisting in a thermally averaging, integrating measuring approach by which the above mentioned thermomechanical parameters can optimally be evaluated.

2- Theoretical Considerations

2.1. General aspects

For many high temperature materials the existence of a protective oxide scales which would enable these materials to survive for a larger period of time under aggressive environment conditions of high oxidation temperatures becomes significant. Regarding the protective effect of such scales several aspects are of marked importance. One of these aspects is the susceptibility to mechanical failure by the presence of thermal stresses in the system oxide scale / substrate. This would mean that even chemically stable and dense protective oxides are quit susceptible to failure in the presence of such stresses. In this aspect, since oxide scales under corrosive conditions are quite brittle, failure would always set on at physical defects- induced stress concentrations sites. This would implement fracture mechanics aspects to solve related failure phenomena. It results that a number of open problems still remain in particular concerning the reliability of thermal stress- strain measurements as well as the correct assessment of critical conditions of mechanical breakdown of protective scales. By the way, there are two main sources of stress formation in the oxide [3-12]:

A. differential thermal stresses induced by different coefficients of (linear) thermal expansion (CTE) and temperature changes in the substrate – oxide system and

B. internal stresses resulting from oxide growth. [In this case one should distinguish between intrinsic growth and geometrically induced stresses]. Thermal stresses are a principal source of mechanical breakdown of protective scale. Thus, when the CTE of scale (surface layer) and substrate may be determined, the resulting differential strain and consequently the associated stresses can easily, theoretically be calculated as a function of range of temperature changes, ΔT. Furthermore, a poor adherence in the interface between substrate and scale may create new surfaces and introduce a thermal barrier and hence thermal gradient ΔT which in turn would lead to additional internal stresses $6_{\Delta T}$ and respective strains, $\varepsilon_{\Delta T}$.

Thus the breakdown behavior is determined mainly by the sum of all stresses formed in the scale i.e.: $6_{tot} = 6_{th} + 6_{grw} + 6_{\Delta T}$ where 6_{th} and 6_{grw} are thermal and intrinsic growing stresses respectively. Similarly, for the respective strains one can put:$\varepsilon_{tot} = \varepsilon_{th} + \varepsilon_{grw} + \varepsilon_{\Delta T}$.

Thus, one can deduce that an improper oxide preparation i.e. a presence of rough and not carefully cleaned substrate surfaces could lead to local failures in form of spalling and/or cracking followed by associated global stress release phenomena in the oxide, fact which would cause an associated global disturbance of the oxide stress – strain state given by the above stress-strain relationships. Since the primarily involved oxide parameters $(E_{ox},\propto_{ox},V_{ox})$ to be evaluated are thermomechanically coupled with the above mentioned state (see next section), such a disturbances would lead to wrong thermal expansion measurements of these parameters.

2.2 Thermomechanical Modeling

In the sketch of Fig (1) a thermally expanding – contracting multisubstrate – structured material system is described. For the demands of the present study, in this system the first – top layer was chosen as a reference magnetic layer of Nickel metal characterized by the paar $(E_o,\propto_o)$ and thickness$t_o = t$. Moreover, this reference layer acts as a relevant stress (strains) sensor by which, in connection with a suitable electronic Micromagnetic Barkhausen Measuring (MBE) device, the desired data are captured and processed. Bearing in mind this sketch one can argue that, due to the mutual thermal expansion response of substrates, their total differential thermal strain contribution to the reference layer strain is given as:

$$\acute{\varepsilon}_o = \Delta\varepsilon_{0/1} + \Delta\varepsilon_{1/2} + \Delta\varepsilon_{2/3} + \ldots..\Delta\varepsilon_{i-1/i} \quad (1)$$

Here $$\Delta\varepsilon_{i-1/i} = \acute{\varepsilon}_{i-1} = \left(\acute{\propto}_{i_{-1}} - \acute{\propto}_i\right)\Delta T \quad (2)$$

is the net strain in the (i-1)th substance layer due to the contribution of the beneath i-th substrate of the system.

Now, the total – effective stress accumulated during heating/cooling procedure in the

reference layer is given as: $6o = \acute{E}_o \cdot \acute{\varepsilon}_o$ and therefore due to Eq (2) one may approximate a general expression as follows:

$$6o = \sum_{i=1}^{n} \int_{T_1}^{T_2} \left[\left(\frac{E_o(T)}{1-V_o}\right) \frac{(\propto_{i-1}(T) - \propto_i(T))dT}{1+\left(\frac{E_{i-1}}{E_i}\right)\cdot\left(\frac{t_{i-1}}{t_i}\right)\cdot\left(\frac{1-V_i}{1-V_{i-1}}\right)} \right] [\Delta T]^{-1} \cong$$

$$\acute{E}_o \cdot \sum_{i=1}^{n} \left[\frac{(\acute{\propto}_{i-1} - \acute{\propto}_i)\cdot\Delta T}{1+\left(\frac{\acute{E}_{i-1}}{\acute{E}_i}\right)\cdot\left(\frac{t_{i-1}}{t_i}\right)\cdot\left(\frac{1-V_i}{1-V_{i-1}}\right)} \right] \quad (3)$$

In this expression we have:

$\Delta T = T_2 - T_1$= range of the temperature change

$\int_{T_1}^{T_2} \propto (T)\, dT/\Delta T = \acute{\propto}_i$= overall – average CTE of i-th substrate in this range

$\propto_i$ = instantaneous CTE (at a given temperature) of i-th substrate

V_i= (instantaneous) Poisson ratio of i-th substrate

V_o= (instantaneous) Poisson ratio of reference (top) layer

$\acute{E}_i$ = overall – average thermoelastic (plastic) modulus of i-th substrate

E_i= instantaneous thermoelastic plastic modulus

$\acute{E}_o$= overall – average thermoelastic (plastic) modulus of reference (Ni) reference layer

$\int_{T_1}^{T_2} \frac{[E_o(T)/(1-V_o)dT]}{\Delta T} = \acute{E}_o =$ overall-apparent apparent thermo-elastic (plastic) modulus of (Nickel) reference layer, where $E_o(T)$= instantaneous thermoelastic (plastic) modulus of Ni – reference layer.

Regarding the last relationship, it should be pointed out that the so – called apparent modulus would arise due to the existence of a multiaxial stress – strain state caused by the predominant isotropic and uniform thermal expansion effect of the material [13]. As such, one should distinguish between the apparent and "common" modulus which is the ratio of stress to strain only for an uniaxial state. In particular, as demonstrated in the related Appendix-I, the apparent modulus in this study arises due to the existence of dominant equi-biaxial – plain stress measuring conditions.

Furthermore, in this study for the (high) temperature – induced thermal deformation of the reference Ni – metal layer one can reasonably expect the formation of a thermoplastic limiting Poisson ratio given as: $V = V_o \to 1/2$ and hence $\acute{E}_o = 2\acute{E}_{op}$. In this sense for most oxide substrates one can further assume, for simplicity, an effective thermoelastic limiting Poisson ratio as: $V_{ox} \to 1/4$. Furthermore, we denote $\acute{E}_o = \acute{E}_{op}$ =thermoplastic effective modulus defined as the secant to a point of the effective stress versus effective plastic strain of the curve as shown in the sketch of Fig (2).

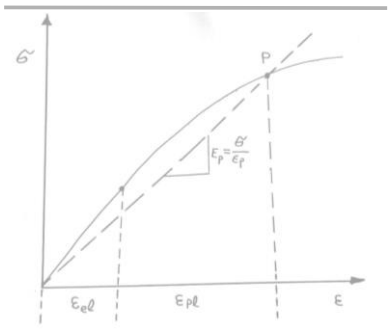

Fig(2): Definition of the plastic modulus, E_p, as the secant modulus to a point on the effective stress versus effective plastic strain ($\varepsilon_{pl} \gg \varepsilon_{el}$)

This means in other words $\acute{E}_{po} = \frac{\acute{6}_{po}}{\acute{\varepsilon}_{po}}$ where $\acute{6}_{po}$ is the effective plastic stress and $\acute{\varepsilon}_{po}$ the respective plastic strain accumulated in the reference (sensor) layer during the cooling of the material system. Now from the general relationship (3) one may obtain of the measuring thermal strains the following relationship:

$$\acute{\varepsilon}_{po} = \frac{\acute{6}_{po}}{\acute{E}_{op}} = \sum_{i=1}^{n} \frac{(\acute{\propto}_{i-1} - \acute{\propto}_i)\cdot\Delta T}{1+\left(\frac{\acute{E}_{i-1}}{\acute{E}_i}\right)\cdot\left(\frac{t_{i-1}}{t_i}\right)\cdot q_V} \quad (4)$$

with $q_{v_i} = (1 - V_i)/(1 - V_{i-1})$.

For example, for the specific cases of present study it is n≤2, which means the existence of a two substrates – structured material system Thereafter, one can put $t_o = t$, $\propto_o = \propto$, $t_s = t_1$, $t_s = t_2$ and obtain finally from Eq(4) the basic formula of the effective thermoelastic – plastic strain developed in the reference layer as:

$$\acute{\varepsilon} = \frac{(\acute{\alpha} - \acute{\alpha}_1)\cdot\Delta T}{1+\left(\frac{\acute{E}}{\acute{E}_1}\right)\cdot\left(\frac{t}{t_1}\right)\cdot q_{V_1}} + \frac{(\acute{\alpha}_1 - \acute{\alpha}_2)\cdot\Delta T}{1+\left(\frac{\acute{E}_1}{\acute{E}_2}\right)\cdot\left(\frac{t_1}{t_2}\right)\cdot q_{V_2}} \quad (5)$$

3. Experimental

3.1.1. Reference sensor layer

In general, the quality of a deposited (thin) material layer depends on the following critical factors [14]:

1- Roughness of substrate surface, **2.** Cleanness of surface, **3.** Substrate temperature and 4. Deposition conditions. Therefore before deposition, the respective substrates were polished with diamond past to achive a minimum roughness between 0, 03 and 0, 05 μm. Afterwards the specimens were cleaned in ultrasonic bath in acetone then in alcohol. The material to be deposited was a Nickel metal (99.5%). This was so because this metal is a quite relevant ferromagnetic material which exhibits a high sensitivity of magnetoelastic response to applied stresses (strains). This is due to its low magnetocristalline anisotropy and large magnetostrictive constant as well as to the existence of four easy axis of magnetization compared to other ferromagnetic materials such as Fe and Co [15].

Consequently, Ni-layer was chosen to act as a magnetic measuring sensor for the thermal stresses (strain) developed in this layer. The preparation of this layer was performed by means of Vapor – deposition performed in a high vacuum of about 10^{-3} – 10^{-4} Torr created within a bell-jar type working chamber, attached to a Edwards – type coating unit. Nevertheless, because of the restrictions imposed, concerning the maximum material quantity permited in the crucible source, required for one – shot evaporation, a thickness of Ni – layer of about 10 μm could be achieved. Nevertheless, one can demonstrate that the emitted MBE- signal needed for the respective measurements is of an acceptable intensity. Furthermore, according to experiences given elsewhere [15] the substrate temperature also plays an important role. In this aspect the respective conditions are fulfilled in the present study in the sense that all the substrates are heated at temperature >Tm/3, with Tm ≅1450C^{o} melting point of Nickel. In the manner, this condition also allows to obtain a layer with vanishing intrinsic growing stresses and an optimally crystallizing microstructure [14].

Following the experiences in [15] a perpendicular beam incidence with the target-substrate surface was chosen to avoid formation of texture-like magnetic microstructures in the vapor condensed Ni-material which would lead to undesired magnetic anisotropy phenomena. Furthermore, to reduce the formation of thermal shock residual stresses, a relative slow cooling rate was involved. This was done by activation of an automatic valve control at the instant of the end of vapor deposition process by alloying a regulated air flow into the vacuum chamber and so a maximum cooling rate of about 1500C^{O}/h. Nevertheless, as a precaution, the sensor layers prepared in this manner, were afterwards carefully examinated by SEM for eventual damages. Thus, no features of microcracking, spallation and buckling could be detected.

3.1.2. Oxide substrate

A). Titanium exists in two allotropic modifications:

Hcp- structured, a-phase and bcc- structured, b-phase. At the critical point T=882C^{o} a transition occurs between these phases. As such, it would be of certain interest to try to evaluate the overall CTE of Titanium in the temperature range above this transition point. Furthermore, oxidation of titanium may be quite complex in forming several stable oxides such as: Ti_2O, TiO, T_2O_3, Ti_3O_5, and TiO_2 [4, 16]. This means that thermodynamically one would expect that oxide scales to consist of the above different titanium oxides. Nevertheless, many studies have been confined to temperature below 1000C^{0} and in most cases the oxidation has been carried out in air or oxygen at *Typeequationhere.*atmosphere pressure. Under these conditions only TiO_2 (Rutile) is formed. The TiO_2 formed during parabolic kinetic rate of oxidation, was initially compact and protective, but after prolonged exposure, at certain critical thickness, the scale mostly cracked and / or spalled. In this sense it is experienced, by many researches, values of

wight gain corresponding to the critical thickness, $t_{cr,}$ at about 750 $C^{o,}$ as 3 $mg/cm^{2.}$ Based on this value and by means of the formula $3mg/ (cm2. t_{cr)} = 6 TiO_{2,}$ a 'theoretical' critical thickness of about 7, 5 μm can be calculated. In the present study a commercially pure Titanium (99, 5%) was used for the oxidation procedure and afterwards tested. The oxidation was performed following the experiences on certain measuring conditions and related indications given in [5, 12].

Consequently, the optimal oxidation conditions were chosen to be: $750C^{o}$ and oxygen pressure 1Atm where a practical parabolic kinetic rate constant $K= 9X10^{-10}.g^{2}. Cm^{-4}. Sec^{-1}$ was abstained. In this sense one can demonstrate that for oxidation times larger than about 8 hrs. Corresponding oxides of thickness larger than about 10μm may be produced. Such oxides, however, presented damage features in form of microcracking spalling and decohesion as revealed by detailed SEM- observations. The so abstained oxide thickness was measured by the classical gravimetric technique by means of a high- precision balance ($-+10^{-4}$ g). The desired optimal values of oxide thickness required for the purpose of present steady are given in section 3.4.

B.) Lanthanum manganities ($La MnO_3$) is a ceramic cell component of a high- temperature solid oxide fuel cell (SOFC) generators, used as electric current collector between the cathode and separator. Thus, the $La MnO_3$-based cathodes include manganese oxides components such as Mn_2O_3 and Mn_3O_4 in order to prevent solid – state reactions during fabrication and operations of thermal cycling under oxidizing atmospheres. However, SOFC configurations are often imposed to significant limitations due to their weak and brittle thermomechanical properties. In order to reduce the thermal stresses in the SOFC generator, a better understanding of thermal expansion behavior of their components is needed. Therefore, reliable experimental evaluations of the CTE of manganese oxide Mn_3O_4 would be of importance. This is because the CTE of this oxide exhibits a quite anomalous behavior with temperature and as such its exact evaluation within given thermal ranges would be difficult. Commercially pure manganese was used in this study, As in the case of Ti , the required oxidation procedure was done by following the experience given in [5,12].

Thermodynamically, one would expect the oxide scale to consist of several layers of different manganese oxides, such as MnO, Mn_3O_4 and Mn_2O_3, however, oxidation in oxygen at near atmospheric pressure and below about $900C^{o}$, only Mn_3O_4 is formed, [17].

Thus the oxidation was performed at $800C^{o}$ and oxygen pressure of about 1Atm. It was so observed that manganese oxidation occurs giving a parabolic rate constant $K"\cong 3.10^{-8}g^{2}.cm^{-4.} Sec^{-1}$ which is higher compared to Titanium. As such, it is much easier to obtain a larger number of oxide thicknesses of various values needed in this study. Indicative SEM-observation resulted in almost no features of damages in form of microcracking, spallation or decohesions. The relevant- optimal thickness values required for the present measurements are given in section (3.4) of this study.

3.2. Master Curve (MC)

A specimen made of Ni (99, 5%) material having a dog-bone like shape was used for this scope. The dimensions were as follows: gauge length = 100mm, width =20mm and thickness 1mm. Before testing the specimen was subjected to an adequate furnace annealing procedure at $600C^{o}$ for 1h, for stress relief. The subsequent tensile test was performed by means of an Instron - type machine at a low strain rate of about $10^{4}/s$.

During the test the stress/ strain as well as magnetic sensor data were taken simultaneous. The magnetic data were abstained by means of a suitable MBE= probe conveniently attached to the tensile specimen surface. The data were taken at given loading steps and afterwards optimally processed for the master – curve (MC) construction. The magnetic data processing was made by an inherent PC component of a respective electronic apparatus set-up. (See next section). In addition to the above – mentioned standard Ni specimen, a second standard one was prepared. This consisted of a sintered MgO material substrate

on which a Ni – layer of 10μm thickness was deposited under the same conditions as earlier described in section 3.1.1. This was so because the CTE values of Ni and MgO present the smallest difference within the required thermal ranges compared to all the other materials involved in this study. In this manner, on cooling to room temperature, acceptable low differential residual thermal stresses are developed. Furthermore, by the following stress relief annealing procedure quite vanishing residual thermal stresses could be measured in the reference Ni - layer. Thereafter, the construction of the required basic Master Curve (MC) was made as follows. MBE -data, taken from the tensile test standard specimen, denoted as Bi, were reduced to the magnetic initial data at zero load B_0 i.e. $\acute{B}_i = \frac{Bi}{B_o}$. At the same time the MBE – data taken from the actually measuring specimens of thermal expansion, denoted as b_i, were reduced to the magnetic data for zero stress taken from the second standard specimen, b_0, i.e. $\acute{b}_i = \frac{b_i}{b_o}$. Thereafter, a MC consisted of a plot of $\acute{B}_i$ versus the corresponding tensile strain, ε_i, was constructed. Now when a $\acute{b}_i$ value is found to (almost) coincides with a $\acute{B}_i$ value and viceversa, i.e. if $\acute{B}_i \cong \acute{b}_i$, then by means of the constructed MC, one can find the associated - expected thermal expansion strains by making tensile strain = $\varepsilon_i \equiv \varepsilon_{th}$= thermal strain and similarly tensile stress= $6_i \equiv 6_{th}$ = thermal stress. The respective detailed procedure is described schematically in the sketch of Fig (3).

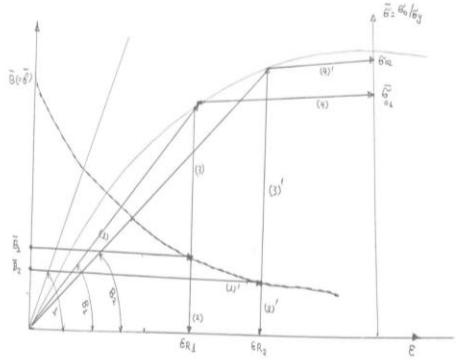

Fig(3) *Sketched procedure of MC-aided data extraction (-) uniaxial tensile curve (- - -) MBE-curve, (1) -> (2) -> (3) -> (4) and (1)' -> (2)' -> (3)' -> (4)' are the consecutive directional steps of data extraction.* ε_{R1} *and* ε_{R2} *are the measured residual thermoplastic strains and* 6_{o1} *and* 6_{o2} *the respective stresses.* $\acute{E}_{op}^{(1)} = tan\beta_1, \acute{E}_{op}^{(2)} = tan\beta_2$ *are "residual" – plastic moduli;* ($\acute{E}_{op}^{(1)} > \acute{E}_{op}^{(2)}$)*, and* $E_o = tan \propto$ *= elastic modulus.*

For instance, as seen in this figure, these strains can primarily be evaluated following the directional steps (1)→ (2). Thereafter, the associated thermoplastic moduli and residual stresses may secondarily be evaluated following the directional steps (1)→ (3) and (1)→ (3) → (4) respectively. In addition, from the same figure the following relationships may be extracted: Young's modulus=tan$a = E_o > tan\beta 1 = \acute{E}_{po1} > tan\beta 2 = \acute{E}_{po2}$, where $\acute{E}_{po1}$ and $\acute{E}_{po2}$are the thermoplastic moduli for Ni – layer. This procedure was applied to the MC of Fig 4 for the data extraction. It is noted that by using the above reduced magnetic the resulting random errors could by far be reduced. It is also noted that by the above basic relationship$\acute{B}_i = \acute{b}_i$, it is reasonably assumed that the magnetic and mechanical properties of bulk Nickel and Ni – layer specimens should be very similar [15].

3.3. MBE – principle and set-up

Nowadays MBE measuring technique is widely used as a magnetic testing tool for evaluation of internal stresses (strains) in ferromagnetic materials. This technique is based on a quite complex micromagnetic phenomenon consisting in domain wall dynamic processes taking place in such materials [18]. The technique is quite sensitive to elastic and plastic residual deformations of these materials and as such may contribute to their mechanical and microstructural characterization [19-21]. In other words, MBE is the magnetic response of the material to externally applied stresses as well to internally existing residual stresses. This response is detected in form of noise signal of a stochastic nature, which, after respective electronic processing, is transformed to the measured discrete electric pulses or energetic counts. The MBE techniques may be used in two basic measuring modes: noise

voltage energy and average count number. The first is given as a root – mean – square voltage profile averaged over given times of sweeps of externally applied magnetic field. In our case the magnetic field was swept from – 0.02T to + 0.02T (= 200 Oe) in a triangular wave form with a frequency of 10Hz.

The Barkhausen noise voltage was amplified by a low-noise preamplifier followed by a band-pass filter with a frequency range from 500 Hz to 100 kHz and transferred to a 16-bit AD board built in an another PC. The detecting coil in the measuring probe had 1000 turns. In the view of the above-mentioned it should be noted that Ni – material used exhibits a much better MBE – response to stresses compared to Fe and as such was a prime sensor candidate for the purpose the present measurements (see Appendix III). Further related details on the MBE – set up and principle are given in [21] and Appendix III.

3.4. Measuring - Evaluation Procedure

3.4.1. Empirical CTE – approximations

I – General

At first one may approximate as follows:

$$\acute{\alpha}\,(\Delta T) = \int_{T_1}^{T_2} \alpha\,(T)\,dT/\Delta T \quad (6)$$

where $\Delta T = T_2 - T_1$, $\alpha\,(T)$= instantaneous CTE, and $\acute{\alpha}\,(\Delta T)$= overall – average CTE in the given thermal range ΔT. Consequently, when an analytical expression of CTE with temperature is given, then the CTE can be evaluated empirically by Eq (6). For instance, many experimentally measured CTE can analytically be approached by a parabolic expression in form:

$$\alpha\,(T) = \alpha_o\,(1 + bT + cT^2) \quad (7)$$

Where α_o is the given CTE at $T = T_R$ = room temperature and b, c constants of best fitting of the above expression to the respective experimental data. Thereafter, one may proceed as follows:

$$\acute{\alpha}\,(\Delta T) = \alpha_o\left(T + \frac{b}{2}T^2 + \frac{c}{3}T^3\right)/\Delta T = \alpha_o\left[1 + \frac{b}{2}(T_2 - T_1) + \frac{c}{3}(T_2 - T_1)^2\right] \quad (8)$$

Further, for $T_2 \gg T_1$ results $\Delta T \cong T_2 = T$ (9)

Thus $$\acute{\alpha}\,(\Delta T) = \acute{\alpha}\,(T) = \alpha_o\left(1 + \frac{b}{2}T + \frac{c}{3}T^2\right) \quad (10)$$

For a linear behavior Eq (10) becomes

$$\acute{\alpha}\,(T) = \alpha_o\left(1 + \frac{b}{2}T\right) \quad (11)$$

and Eq (7):

$$\alpha\,(T) = \alpha_o\,(1 + bT) \quad (12)$$

II – Specific

A) For Titanium a linear behavior with temperature of its CTE in the range ΔT= (0-700) ℃ was observed [22]. By the measurement data given in that reference and for a given $\alpha_o = 8.5 \times 10^{-6}/℃$ and applying a best fitting procedure, the constant b of Eq (11) can be calculated as:
$b \cong 6.1 \times 10^{-4}$
Consequently, by eq (12) one may obtain $\alpha_{Ti}\,(700℃) = 12.5 \times 10^{-6}/℃$, and by Eq (11) $\acute{\alpha}_{Ti}\,(\Delta T = 700℃) = 10.5 \times 10^{-6}/℃$

B) For high-density sintered magnesia, MgO, (98%) the experimental data in [23] gives a non-linear behavior of CTE with temperature. Hence, for a given $\alpha_o = 6.5 \times 10^{-6}/℃$, by Eq(7) one may obtain the fitting constants as $b = 1.1 \times 10^{-4}$ and $c = -1.5 \times 10^{-7}$
Consequently, one can obtain by Eq (10)
$\acute{\alpha}_{MgO}\,(\Delta T = 1400℃) \cong 11.6 \times 10^{-6}/℃$
And by eq (7) $\alpha_{MgO}\,(1200℃) = 12 \times 10^{-6}/℃$

C) For Ni (nickel) the experimental data given in [24] present an almost linear behavior of CTE with temperature. As such the fitting constant are calculated:
$b = 5.1 \times 10^{-4}$
Consequently, one may obtain, by Eqs (11) and (12), $\acute{\alpha}\,(\Delta T) \cong 17 \times 10^{-6}/℃$ and $\alpha\,(1400℃) \cong 22 \times 10^{-6}/℃$ respectively. (For $\Delta T \cong 1400℃$ and a given $\alpha_o = 12.5 \times 10^{-6}/℃$)

3.4.2. Empirical Approximation of thermoelastic Young's Modulus

In [25] a universal expression of instantaneous elastic Young's Modulus in function of temperature was established in form of:

$$\frac{E(T)}{E_o} = 1 - 0.2\left(\frac{T}{T_{melt}}\right) - 0.25\left(\frac{T}{T_{melt}}\right)^2 \quad (13)$$

Where $E_o = E(T = 0℃)$

Thereafter, for $\Delta T = T_2 - T_R \cong T_2 = T$, $(T_2 \gg T_R)$ one may approximate:

$\acute{E}(\Delta T) = E_o \int_{T_R}^{T_2} E(T)\, dT/\Delta T = E_o \left[1 - \frac{0.2}{2}\left(\frac{T}{T_{melt}}\right) - \frac{0.25}{3}\left(\frac{T}{T_{melt}}\right)^2\right]$ = overall-average thermoelastic modulus in the given temperature range ΔT.

Especially, for Ni one can estimate this modulus in the range $\Delta T = T_m - T_R \cong T_m$ = 1450℃= melting point of Nickel as:

$$\acute{E}\ (\Delta T) = E_o \times 0.8 = 200GPa \times 0.8 = 160GPa$$

3.4.3. Overdeterministic measuring approach

3.4.3.1. Substrate temperature variation

A) Partial cooling

By means of the basic relationship (5) one obtains for n=1 and $t \ll t_1 = t_s$, the following expression of partial cooling procedure:

$$\acute{\varepsilon} = \left(\propto^{\acute{(1)}} - \propto_s^{(1)}\right)\Delta T_1 + \left(\propto^{\acute{(2)}} - \propto_s^{\acute{(2)}}\right)\Delta T_2 \quad (14)$$

With $\Delta T_1 = T_m - T_s$ and $\Delta T_2 = T_s - T_R$ and T_m = melting point of Nickel (= 1450℃), T_s = substrate heating temperature, T_R = room temperature (=20℃).

$\propto_s^{(1)}$ = instantaneous CTE of substrate at T_s

$\propto_s^{\acute{(2)}}$ = overall – average CTE of substrate in the cooling range ΔT_2

$\propto^{\acute{(1)}}$ = overall – average CTE of Ni surface layer in the cooling range ΔT_1

$\propto^{\acute{(2)}}$ = overall – average CTE of Ni – surface layer in the cooling range ΔT_2

Furthermore, by means of Eqs (11), (12), one obtains:

$$\propto^{\acute{}}\ (\Delta T) = \propto_o \left(1 + \frac{b}{2}T_m\right), \quad (\Delta T = T_m - T_R \cong T_m) \quad (15)$$

$$\propto^{\acute{(1)}} = \propto_o \left[1 + \frac{b}{2}(T_m - T_s)\right], \quad (\Delta T_1 = T_m - T_s) \quad (16)$$

$$\propto^{\acute{(2)}} = \propto_o \left(1 + \frac{b}{2}T_s\right), \quad (17)$$

It is noted that T_s is at the same time the temperature at which Ni – vapor condenses on the substrate surface and in this sense $\Delta T_1 = T_m - T_s$ can also be seen as a vapor "condensing" range. In addition, T_s is the temperature at which both surface Ni – layer and substrate material begin simultaneously to cool down toT_R.

B. Standard substrates

For demands of Eq (14) two standard substrate specimens are considered as follows:

$\propto_{s1} = \propto_{mul}^{(1)} \cong \propto_{mul}^{\acute{(2)}} = 5.5 \times 10^{-6}/℃$,

$\propto_{s2} = \propto_{SiO_2}^{(1)} \cong \propto_{SiO_2}^{\acute{(2)}} = 0.5 \times 10^{-6}/℃$,

The first is Mullite $(3A_2O_3 \cdot 2SiO_2)$ and the second is Silica glassSiO_2. This is because these materials show very stable CTE with large temperature changes [23].

C. Measuring proceduse

C1. Ni-layer

Frequently, the use of deterministic methods may become inappropriate, because errors in the measurements could introduce large errors in the determination of the unknown parameters. To avoid such errors additional number of measurements should be made so that the amount of data available exceeds the number of unknowns by factor of 2 or more. With this additional data, overdeterministic solutions for the results are improved by statistical averaging in a least – square sense performed by numerical best fit procedure. Thus, by means of the above presented relationships (14) of measuring procedure the conditions of overdeterministic approach can be fulfilled. As such, by making combined measurements for two given $T_s = 700℃$ and $T_s = 1450℃$ as well as two substrates$\propto_{s1} = \propto_{mull}, \propto_{s2} = \propto_{SiO_2}$, one can perform four (4) measurements for the determination of the single unknown $b = b$. This can be calculated after substitution of Eqs (15), (16), (17), into eq

(14) and obtaining a linear systems of "b". As such, an overdeterministic factor of 4 results. The crucial step now would consist in comparing the so calculated value of $\acute{\alpha}^{(1)}$ and $\acute{\alpha}^{(2)}$ with that obtained for Ni by the empirical approximation procedure presented in section 3.4.1. – C. As such, the degree of discrepancy between these values can be seen as a measure of reliability of the above proposed overdeterministic measuring approach. It is remembered that the value of the constant b in that section was calculated by best fitting on the experimental data obtained by X – ray diffraction and dilatometry technique [24]. In other words, in this manner reliability of the present experimental technique, compared to X-ray diffraction and dilatometry, can also be estimated.

C2.Titanium substrate

Similarly to the case of Ni – layer, one can obtain from Eq. 14:

$$\acute{\varepsilon}_o = \left(\alpha^{\acute{(1)}} - \alpha_{Ti}^{(1)}\right)\Delta T_1 + \left(\alpha^{\acute{(2)}} - \alpha_{Ti}^{\acute{(2)}}\right)\Delta T_2 \quad (18)$$

By Eqs (11, 12) and for a linear behavior of Titanium, one obtains

$$\alpha_{Ti}^{(1)} = \alpha_o\,(1 + b \cdot Ts) \text{ and } \acute{\alpha}_{Ti}^{(2)} = \alpha_o\left(1 + \frac{b}{2} \cdot Ts\right) \quad (19)$$

After substitution of equations (19) and Eqs (16), (17), for$\acute{\alpha}^{(1)}$ and$\acute{\alpha}^{(2)}$, into eq (18) and bearing in mind that the constant $b = b$ for nickel is well determineted, certain linear systems in function of $b = b_{Ti}$ corresponding to the number of measurements made by substrate temperature $T_s = 600℃$, $T_s = 1000℃$ and $T_s = T_m = 1455℃$. Are obtained .As such, an overdeterministic factor of 3 results.

C3. Magnesia Substrate (MgO)

In a way similar to that of Ni – reference layer of Eq. (14) one obtains:

$$\acute{\varepsilon}_o = \acute{\varepsilon} = \left(\acute{\alpha}^{(1)} - \alpha_{MgO}^{(1)}\right)\Delta T_1 + \left(\acute{\alpha}^{(2)} - \alpha_{MgO}^{(2)}\right)\Delta T_2 \quad 20)$$

Now, by Eqs (8), (10), due to the earlier mentioned non – linear behavior, one obtains:

$$\acute{\alpha}_{MgO}^{(2)} = \alpha_o\left[1 + \frac{b}{2}(T_m - T_s) + \frac{c}{3}(T_m - T_s)^2\right] \quad (21)$$

$$\acute{\alpha}_{MgO}^{(1)} = \alpha_o\,(1 + bT_s + cT_s^2) \quad (22)$$

$$\acute{\alpha}_{MgO} = \alpha_o\left(1 + \frac{b}{2}T_m + \frac{c}{3}T_m^2\right) \quad (23)$$

It is noted that for $T_s = T_m$ results $\Delta T_1 = 0$ and$\Delta T_2 = \Delta T = T_m - T_R$. $\alpha^{(1)}$and$\alpha^{(2)}$are well-predermined by the constant b_{Ni} through Eqs.(16), (17).

Similarly to the case of Ti, as presented earlier, after convenient substitutions, a linear system in function of two unknowns' b and c for magnesia is obtained. By variation of substrate temperature, for example$T_s = 300℃$,$T_s = 600℃$,$T_s = 1000℃$ and $T_s = T_m = 1455℃$, an over deterministic calculation factor of 2 results. As mentioned in the case of Titanium and Nickel, the so obtained constants (b, c) should be used through the Eqs (7), (10), to obtain the corresponding CTE. The so evaluated CTE will be compared with the CTE, empirically calculated as given in section 3.4.1. The degree of discrepancy between the two CTE will be discussed in terms of a measure of the reliability of the proposed approaches.

D. For the sake of completeness it should be stated the following. By the substrate temperature variation approach from Eq (14) a more general relationship of partial cooling can be established:

$$\frac{\acute{6}_o}{\acute{E}_o} = \acute{\varepsilon}_o = \left(\alpha^{\acute{(1)}} - \alpha_s^{(1)}\right)\Delta T_1 + \left(\alpha^{\acute{(2)}} - \alpha_s^{\acute{(2)}}\right)\Delta T_2 = \acute{\varepsilon}_o^{(1)} + \acute{\varepsilon}_o^{(2)} = \frac{\acute{6}_o^{(1)}}{2\acute{E}_o^{(1)}} + \frac{\acute{6}_o^{(2)}}{2\acute{E}_o^{(2)}} \quad (24)$$

Here the pairs $(\acute{6}_o^{(1)}, \acute{E}_o^{(1)})$ and $(\acute{6}_o^{(2)}, \acute{E}_o^{(2)})$ contain the respective parameters within the partial temperature ranges ΔT_1 and ΔT_2 respectively; concerning the Ni – surface layer. Thereafter, the parameter $\acute{E}_o = \acute{E}_{op}$ should be seen as an equivalent –overall thermoplastic modulus of

Nickel metal, valid within the total thermal cooling range$\Delta T_1 + \Delta T_2 = \Delta T = T_m - T_R \cong T_m = T$. As such this equivalent modulus would be a function of the respective partial moduli $\acute{E}_o^{(1)}$ and $\acute{E}_o^{(2)}$.

E) Furthermore, for Ts=Tm and$\Delta T = T_m - T_R$, the Eq (24) becomes:$\acute{\varepsilon}_{op} = (\alpha_o - \alpha_s)\Delta T$. By this measuring formula and using various, different standard substrate materials as well as the procedure described in Fig (3), the thermoplastic modulus of Nickel can be evaluated-extracted from Fig.4 in function of resulting associated thermoplastic strain.

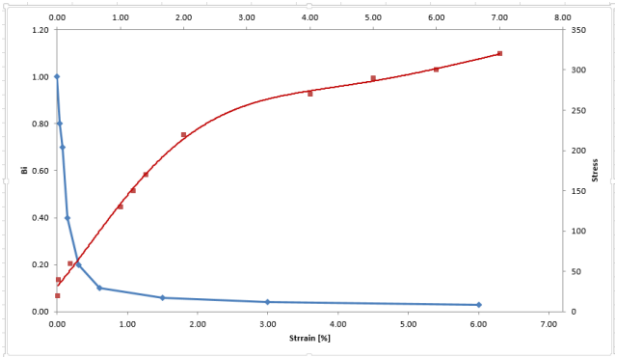

Fig. 4: *Constructed Composite Master Curve consisting of Barkhausen – Strain curve and stress- strain curve.*

The modulus obtained in this way will be discussed in the next section by means of Table 4. The substrate materials needed for these evaluations were Silica glass, Mullite, Titanium and MgO. The last two materials were taken as standard one because their CTE show a well-determined behavior in the given thermal range.

3.4.3.2. Substrate thickness variation

A) From the basic Eq (5), for n=2 and t = commensurable to $t_1 = t_{ox} = t_{TiO_2}$ and $t_{ox} \ll t_{met} = t_{Ti} = t_2$ = thickness of oxidizing metal substrate, one can obtain:

$$\acute{\varepsilon} = \frac{(\alpha - \alpha_{TiO_2})\cdot\Delta T}{1+\left(\frac{t}{t_{TiO_2}}\right)\cdot\left(\frac{\acute{E}}{\acute{E}_{TiO_2}}\right)\cdot q_1} \quad (25)$$

With $\Delta T = T_m - T_R$ and $q_1 = 3/2$

Following the experiences on oxidations conditions presented in section (3.1.2)-A, it was possible to obtain almost damage-free TiO_2 – oxide substrates of thickness: t_1= 1.2 μm, t_2= 2.3 μm, t_3= 4.8 μm and t_4= 9.4 μm.

Denoting now $\frac{\acute{E}}{\acute{E}_{TiO_2}} = A$ and $\alpha_{TiO_2} = B$ in Eq (25) and making four (4) measurements corresponding to the above four different oxide thicknesses, an overdeterministic approach for the two fitting constants A, B of a factor of two (2) is obtained. Before this$\acute{E} = t_{an\beta}$ should be pre-determined by the secant definition described in Fig (2) as well as by means of the MC principle of Fig (3) applied to the MC of Fig (4). Afterwards, one can calculate$\acute{E}_{TiO_2} = \frac{\acute{E}}{A}$, for the needed thermoelastic modulus of Rutile.

B) Also from the basic Eq (5) for n=2 and t commensurable to $t_1 = t_{ox} = t_{Mn_3O_4}$ and $t_{ox} \ll = t_{Mn} = t_2$= thickness of oxidizing metal substrate, one obtains:

$$\acute{\varepsilon} = \frac{(\alpha - \alpha_{Mn_3O_4})\cdot\Delta T}{1+\left(\frac{t}{t_{Mn_3O_4}}\right)\cdot\left(\frac{\acute{E}}{\acute{E}_{Mn_3O_4}}\right)\cdot q_1}$$

with $\Delta T = T_m - T_R \cong T \cong 1400°C$ (26)

Furthermore, taking into considerations the experimental experience on oxidation conditions presented in section (3.1.2 –B), it was possible to obtain, within a maximum oxidation time of about 2 hours, damage-free oxide substrates of thickness t_1= 1.6 μm, t_2= 2.9 μm, t_3= 6.2 μm, t_4= 11.9 μm, t_5= 23.2 μm and t_6= 45.3 μm making so possible an overdeterministic approach of a factor of 3. In a way, similarly to the above – mentioned case ofTiO_2, one can proceed to obtain by Eq. (26) the two unknown constants as:$\frac{\acute{E}}{\acute{E}_{Mn_3O_4}} = A$ and $\alpha_{Mn_3O_4} = B$.

Thereafter, by $\acute{E}_{Mn_3O_4} = \frac{\acute{E}}{A}$ one can finally obtain the required thermoelastic modulus of Hausmannite oxide.

4. Results and Discussion

The first problem to be discussed concerns the scatter of the results. This should be, at first, attributed to the principle of the measuring technique used. As such, the present technique reflects an indirect and relative one, by which the needed parameters are obtained in a thermally-averaging measuring manner, compared to the other existing ones, by which these parameters are obtained in a direct measuring way, step by step with temperature. In this sense, the average scatter of the present technique would be, "per see", not larger than that of the other direct techniques. Nevertheless, there are appreciable variations in the data concerning the overall elastic and/or thermoelastic plastic Young's modulus. Especially the thermoplastic modulus is lacking of detailed experimental data. At the same time there are variations in the existing data on overall CTE and especially on the discrepancies of their temperature range dependence. Additional statistical scatter would be introduced by many factors such as thickness variations of surface layer and/or (oxide) substrate, oxidation conditions (temperature and rate), initial roughness, mechanical behavior and microstructural changes in the substrate/surface layer system. For instance, in the present technique, among others, a thickness-variation measuring approach of the surface layer/substrate system is used. This is made by a gradual reduction of the substrate thickness. As such, it is well-known that the mechanical behavior of a thin material may differ considerably from a thick-balk material. In this aspect "thin" specimens would be more susceptible to stress relaxation phenomena compared to "thick" ones. This would also depend on the respective rates of the stress build-up, creep rate and cooling rate under anisothermal conditions. As explained in the related Appendix II, thickness reduction-induced stress relaxation may considerable alter the stress-strain sate in the reference surface layer and introduce uncontrolled random errors in the measurements. The afore-mentioned items indicate that the obtained results seem to depend primarily on the method used and secondarily on the existing data of the standard parameters used and as such great care must be taken in comparing the respective data obtained.

In Fig (4) the required composite MC is presented. This was constructed in the way described in section (3.2) of this study. Afterwards, the required data of stress, strain and related moduli were extracted following the procedure described in the sketch of Fig (3). As a matter of fact, it is pointed out that in Fig (3) the initially obtained tensile stress-strain curve (1) was well-corrected for the actually dominating measuring conditions of equi-biaxial plane stress state by following the procedure in [13]. The resulting effective-true curve (2) was used, instead of curve (1), for the respective data extraction, following the afore-mentioned procedure of Fig (3). In general, such effective curves are independent of the state of stress and as such may be utilized to estimate-simulate stress-strain curves for various different states of stress [13]. In other words, to do so for a particular material, it is necessary to have the curve for a state of stress, such as the uniaxial tensile one in our case.

Thereafter, by means of the data presented in tables (1) (1-A) and (2), a comparison between the present measured and empirically calculated overall CTE can be made. The empiral calculations were performed, as shown in sections 3.4.1-3.4.2, on the basis of the data found in the cited literature in which the respective techniques used are also described. Indeed, a more detailed examination of the related literature reveals an appreciable number of different formula for calculating the CTE grouped into two basic categories depending on whether the thermal expansion relates to a given temperature range or a single temperature. Both of these groups may thus have quite subtle variations with temperature and the resultant values of the overall CTE might vary significantly according to the definition employed. In this aspect, bearing in mind the possible numerous sources of experimental errors, as mentioned earlier, a relative good agreement between the two data

groups presented in tables (1) (I-A) and (2) can be deduced. In particular, this agreement could be better justified when the earlier mentioned substantial difference between the basic principle of the present technique, as an averaging-indirect one, and the principle of the other techniques, as direct-absolute ones, are taken into considerations.

In table (3) the data concerning the thermomoelastic moduli of the two oxides studied are presented. This table helps in comparing the moduli determined by the present technique with those empirically calculated by the universal formula (13) used, in the text. Again, a relative good agreement between the two data groups can be observed. As such, the uncertainties arise to be between 5% and 8%. Indeed, no other sources of related data for additional comparison could be found. In table (4) the data obtained for the Nickel sensor material, concerning the measured thermoplastic moduli, are presented. The related procedure of evaluations is given in section (3.4.3.1-A). As expected, these moduli decrease with increasing residual-referred strains. In this aspect, in obtaining reduced errors and constructive comparisons, the actual moduli were reduced to the common elastic (Young's) modulus resulting in the ratio of parameter 0≤ "δ" ≤1. Thus, this parameter will decrease rapidly toward values < 1. By the way, the essential meaning of this parameter is that it can be utilized as so-termed reduction factor for determining the slope of the stress-strain curve following plastic yielding point, the slope before this point being the initial elastic Young's modulus, Eo, and after this point being δ. Eo [13]. In this manner a post-yielding analysis approach for the material can be performed, where a measure of its yielding or flow rate can be established. Furthermore, in this aspect it is interesting to comment the expected behaviour in Fig (5) in conjunction with the demonstration given in Appendix- IV.

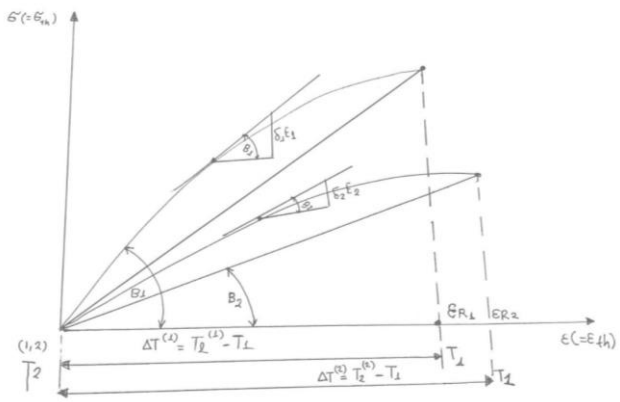

Fig. (5) *Cooling process-determined thermal stress-strain evolution; influence of cooling range (duration) on the thermoplastic modulus.* $(E_1 = tan\beta_1, E_2 = tan\beta_2)$. $T_2^{(2)} > T_2^{(1)}$, *source temperatures of vapor deposition,* T_1=T_R=*room temperature=constant.*

As shown in this Appendix, the related overall – average thermoplastic modulus may appreciably vary with temperature range of cooling resulting in an increase in this modulus with decreasing cooling range. Consequently, the related δ-parameter would also increase with a decrease in the cooling range. From the above-mentioned and bearing in mind the essential meaning of the afore-mentioned δ-parameter, the changes in the stress-strain curves, as illustration in Fig (5), result. Thus, a curve due to the combined effects of residual strain reduction and stress-elevation, would arise. From this, certain opposing effects of residual strain and cooling range changes on the respective overall as well as plastic moduli may also be deduced. As such, from Fig (5) one might expect that the effect would be a net increase in the measured thermoplastic modulus by a reduction in the cooling range ΔT. This would also mean that an increase (a decrease) in the δ-parameter, caused by a respective decrease (an increase) in the cooling range duration, could lead to a thermoplastic hardening (softening) of the material. In general, from Fig (5) it can be argued that the combined effect of a residual strain reduction and stress elevation, induced by cooling range changes, may lead to the above thermoplastic modulus behavior.

In closure, it must be pointed out that by the present technique the respective thermal expansion parameters for materials with larger CTE than that of Nickel metal, can also be evaluated. Such materials could be Cu, Al, Mg, Mn and oxides such as MoO_3. In this situation, compressive thermal stresses are expected to be present in the Nickel sensor layer. This fact implies the construction of a reference MC based on a uniaxial compression test of Nickel bulk material. As such, MBE-signal would increase with applied stress (strain). Furthermore, magnetic materials such as Fe and Co and their (magnetic) oxides could also be included. It results that additional testing procedure should be performed. Thus, the MBE-signal, b1, before and, b2, after Nickel deposition on the tested magnetic specimen surface should separately be measured. b1 is the magnetic signal taken from Ni-layer deposited on a standard specimen such as Mullite or Silica glass. This would mean $\acute{b}_i = (b_2 - b_1)/b_0 = b_i/b_o$ where b_i is the remaining effective MBE-signal obtained after subtracting the intensity of the two signals and b_o is the reference signal as earlier used.

5. Conclusions

In this work a novel experimental technique for the evaluation of thermal expansion parameters of various solid materials has been proposed. Compared to the other existing techniques, the present one represents a rather relative-indirect measuring method by which the respective parameters are obtained using standard materials as well as certain well-established magnetoelastic properties of Nickel material concerning its micromagnetic response to thermomechanical stresses. Thus, it can be demonstrated that the sensitivity of this response is appreciable high in order to detect and measure small changes in the thermoplastic strains developed within predetermined thermal cooling ranges. In this sense the proposed technique arises to be a thermally averaging measuring method for the related parameters. As such, the overall-average thermal expansion-parameters may primarily be evaluated. For this scope a relevant thermomechanical modelling approach-coupled measuring procedure was involved by which the desired CTE and related thermoelastic-plastic moduli, could optimally be evaluated. The testing materials involved were three types of metallic oxides (Mn_3O_4, TiO_2, MgO) as well as two types of metals (Ni, Ti). Owing to the simplicity of the modelling of the theoretical as well as experimental approaches the results obtained seem to be in a reasonable agreement with those evaluated by data found in the existing related literature. Furthermore, using a modelling approach to the cooling range-influenced evolution of thermoplastic modulus, a thermoplastic hardening/softening effect on the Ni sensor maerial could be expected. For instance, it can so be demonstrated that an increase (a decrease) in the thermal cooling range would lead to an associated thermoplastic softening (hardening) of the material. Although the proposed technique is a convenient, reliable and versatile measuring approach, it arises to be labor-and time consuming in properly preparing the specimens. Nevertheless, the technique seems to be, at least from an academic viewpoint, a promising complementary method for optimal evaluation of thermal expansion parameters of solids.

References

[1] D. James, J.A. Spittle, R. Evans “A “,review of measurement techniques for the thermal expansion coefficient of metals and allows at elevated temperatures “,Meas. Sci. Techno l. 12 R1, 2001.N. B

[2] ASTM-E228-22 (i). Standard Test Methods for Linear Thermal Expansion of Solid Materials with push- Rod Dilatometer, (2023).

[3] Michael Schutze, “Failure of Oxide Scales on Advanced Materials due to the presence of Stresses “, in proceedings of Workshop on High Temperature Corrosion of Advanced Materials and protective Coating, Tokyo, Japan, December 5-7, (1990).

[4] A.S. Khana, “Introduction to High Temperature Oxidation and Corrosion “, ASM-International, the Materials Information Society, (1999).

[5] K. Haufe, “Oxidations von Metallen und Metallegieungen”, Springer- Verlag, Berlin / Gottingen/Heidelberg, (1956), (in German).

[6] A. M. Huntz, "Stresses in NiO, Cr_2O_3 and A_2O_3 Oxide scales ", Mat. Sci., Engn. : A, vol 201, issue 1-2, (1995), pp.211-218.
[7] N. Birkens, G. Meier, "Introduction to high temperature oxidation of Metals", Cambridge Univ. Press, (2006) (2end edition).
[8] D.J. Joung, "High Temperature Oxidation of Metals ", Elsevier Ltd., (2016).
[9] U.R. Evans, "The Corrosion and Oxidation of Metals", Arnold, (1960).
[10] J. West "Basic Corrosion and Oxidation of Metals, "Ellis Horward Ltd., (1980).
[11] O. Kubasehewski, B.E. Hopkins "Oxidation of Metals and Alloys", London, Butterworths, (1962).
[12] Karl. Hauffe, Oxidation of Metals, plenum Press. New York [1965].
[13] N. E. Dowling, "Mechanical Behaviour of Materials; engineering methods for deformation, fracture, and fatigue", Prentice- Hall Int. Ed. (1993).
[14] Rene A. Haefer, "Oberflachen – und Dunnschicht-Technologie; TeiI: Beschichtungen von Oberflachen ", WFT: Ed. B.Ilschner, Band 5. (In German). Berlin, Heidelberg; New York, London; Paris; Tokyo: Springer. (1987).
[15] L. W. Kirenski, "Magnetismus", (Kleine naturwissenschaftlice bibliothec, Reihe physike .Band 9, BSB B.G. Teubner Verlagsgesellschaft, Leipzig, 1969.
[16] P. Kofstad, "High temperature Oxidation of Titanium", J. of Less Common Metals , vol 12 issue 6 , pp 449 -464, (1967).
[17] Nasashi Mori, "Expansion Behavior of $Mn_3O_{4+\delta}$Spinel and shrinkage behavior of $La_{0,6}$ $Sr_{0,4}$ MnO_3Composites with Spinel during thermal cycling in O_2 atmosphere", Proceedings of Electro-chemical Society, PV 2001-16,pp 641-649, (2001).
[18] S. Chikazumi, "Physics of Magnetism ", John Wiley & Sons, Inc. New York, London. Sydney, (1964).
[19] L. B. Sipahi, "Overview of application of micromagnetic Barkhausen emissions as noninvasive material characterization technique", J. Appl. Phys., vol.75, pp: 6978-6980, (1994).
[20] C. G. Stefanita, D. L. Atherton, L. Clapham, "Plastic Versus elastic deformation effects on magnetic Barkhausen noise in steel ", ACTA Materialia, vol. 48, pp. 3545-3551, (2000).
[21] E. K. Ioakeimidis, V.N. Kytopoulos and E. Hristoforou, " Investigation of magnetic, mechanical and microfailure behavior of ARMCO-type low carbon steel", Mat. Sci. Eng., A, vol. 583, pp585-592, (2013).
[22] Peter Hidnert, Research Paper RP1520, part of Journal of Research of National Bureau of Standards, vol.30, February 1943, pp 101-105.
[23] J. F. Shackelford, "Introduction to Materials Science for Engineers", 5th Ed., Prentice Hall Inc. upper Saddle River, New Jersey 07458, (2000).
[24] C. Liu, A. M. Huntz, E. Jolles, J.L. Lebrun, "The Influence of Cooling Temperature on the Residual Stresses in the Ni- NiO System" J. Mat. Sci. Letters 11, pp1667-1670, (1992).
[25] D. Zakarian, A. Khachatrian, S. Firstov "Universal Temperature Dependence of Young's Modulus ", Metal Powder Report, Vol. 74, No4, (2019).
[25] H. Nishihara, S. Taniguchi, I. Oguro, M. Harada, T.Ogino, S. Matsumoto, Y. Shindo and N. Ohtsuka: "The Effect of Mechanical Stress on Barkhusen noises from Heat – Treated Nickel Plates "12th A-PCNDT 2006-Asia – Pacific Conference on NDT, 5th – 10th Nov 2006, Auckland, New Zealand.
[27] R. K. Kirby: "Thermal Expansion of Rutile from 100 to 700 C^o ", J. of Research of N.B. of Standards – A. Physics and Chemistry, Vol. 71A, No.5, (1967), pp363-369.

Contribution of Individual Authors to the Creation of a Scientific Article (Ghostwriting Policy)

The authors equally contributed in the present research, at all stages from the formulation of the problem to the final findings and solution.

Sources of Funding for Research Presented in a Scientific Article or Scientific Article Itself

No funding was received for conducting this study.

Conflict of Interest

The authors have no conflicts of interest to declare that are relevant to the content of this article.

Appendix I

Multiaxial thermal stress-strain state

In an isotropic and homogeneous material uniform thermal stresses/strains expansion may occur in all directions and therefor the Hooke's law for three dimensional elastic deformation can be generalized to include thermal effect in form [13]:

$\varepsilon_x = \frac{1}{E}\left[6_x - V\left(6_y + 6_z\right) + \propto \cdot \Delta T\right]$
(I-a)

$\varepsilon_y = \frac{1}{E}\left[6_y - V(6_x + 6_z) + \propto \cdot \Delta T\right]$
(I-b)

$\varepsilon_z = \frac{1}{E}\left[6_z - V\left(6_x + 6_y\right) + \propto \cdot \Delta T\right]$
(I-c)

where V = Poisson ratio and E = Young's modulus of elasticity, $\propto$ = CTE and ΔT = thermal expansion rage.

In absence of shear stresses the in – plane x, y, axis' are the principal ones and for equi-biaxial stress/strain state also $\varepsilon_x = \varepsilon_y$ and$6_x = 6_y$. However, for (very) thin specimens of Ni – layer, one can assume $6_z \approx 0$ and as such for in-plain measuring conditions the last of the above Eqs concerning the through-thickness measurements, should be omitted.

With respect to the above relationships, it is noted that if a free thermal expansion is prevented by various geometric as well as physical constraint factors, then a sufficient thermal change ΔT would cause large thermal stresses of practical engineering importance. Especially, in the present case this may happen due to the mutual constraint conditions of substrates and surface Ni – reference layer. Thereafter, from the above Eqs (I-a) and (I-b), one obtains:

$\varepsilon_x = \frac{1}{E}\left[6_x - V6_y + \propto \cdot \Delta T\right]$
(I-d)

$\varepsilon_y = \frac{1}{E}\left[6_y - V6_x + \propto \cdot \Delta T\right]$
(I-e)

and further, after simple manipulations:

$6_x = 6_y = \left(\frac{E}{1-V}\right) \cdot \propto \Delta T = 6_{th}$= thermal stress
(I-f)

which means

$6_{th} = E_{ap} \cdot \varepsilon_{th}$
(I-g)

valid for the thermoelastic stress-strain behavior, where $\acute{E}_o = E_{ap}$ = apparent Young's modulus given as$\frac{E}{(1-V)} = E_{ap}$.

Furthermore, for thermoplastic stresses/strains one can expect: $V_o \to 1/2$ and consequently, Eq. (I-g) becomes:

$6_{th}^{(P)} = 2E_p \cdot \varepsilon_{th}^{(P)}$, with $2E_p = E_{ap} = \acute{E}$ apparent thermoplastic modulus of Ni-layer.

Appendix II

Stress relaxation approach

Long-term stressing especially at elevated temperature, can convert part of the resultant elastic deformation into plastic one, without altering the overall degree of initial deformation. That gradually reduces the initial stress at first rapidly and then at a constant decay rate. In this sense stress relaxation phenomenon is in effect one of the extreme forms of creep phenomenon under the action of variable stressing.

The resultant deformation, however, is affected by the previous stressing of the material. Resultant plastic deformation may cause various microstructural damages and their effects are superimposed on those of temperature changes and time of thermal exposure. Clearly, the rate and effects of relaxation grow (fall) rapidly with the increase (decrease) in the temperature.

Obviously, relaxation is an essential factor to be taken seriously in thermal oxidation practice. For this scope the denumerator of basic Eq (5) in the following is considered for n=1:

$$1+\frac{t\ \acute{E}\ /(1-V_o)}{t_{ox}\cdot\acute{E}_{ox}/(1-V_1)}=1+\frac{t\ \cdot\acute{E}_{ap}^{(\ )}}{t_{ox}\cdot\acute{E}_{ap}^{(ox)}}\cdot\left(\frac{3}{2}\right)$$

(II-a)

(for $V_o \to 1/2$ and $V_1 \to 1/4$)

Thus, the product of thickness X modulus is expressed in dimension of $[m]\times\left[\frac{GPa}{m^2}\right]=\frac{GPa}{m}=$ force per unit length = specific force, F. This force, under relaxation conditions, becomes

$$\acute{F}=F_o exp\left[-c\left(\frac{t_r}{n}\right)\right],$$

(II-b)

c = constant, t_r = relaxation time, n = apparent viscosity, F_o = initial unit force (amplitude). Consequently, the expression (II-a) becomes under relaxation conditions

$$1+\frac{F_o^{(\ )}exp\left[-c_1\left(\frac{t_r}{n_1}\right)\right]}{F_o^{(ox)}exp\left[-c_2\left(\frac{t_r}{n_1}\right)\right]}$$

(II-c)

The apparent viscosity falls steadily with increasing stress and can be approximated [13]:

$n=1/B\cdot F_o^m$ with m>1

Now, after some manipulations, expression (II-a) becomes:

$$1+\frac{F_o^{(\ )}}{F_o^{(ox)}}exp-\left[c_1B_1F_o^{m(\ )}-c_2B_2F_o^{m(ox)}\right]\cdot t_r\cdot(3/2)$$

(II-d)

and further, a more general final form:

$$1+\acute{F}_o exp-\left[\frac{t_r}{\epsilon_c}\right]$$

(II-e)

with $\acute{F}_o=F_o^{(\ )}/F_o^{(ox)}$ = effective mutual amplitude and $\epsilon_c=\left[c_1B_1F_o^{m(\ )}-c_2B_2F_o^{m(ox)}\right]^{-1}$ = mutual decay rate constant. The expression (II-e) might be interpreted as follows: a gradual reduction in the oxide initial substrate thickness would rapidly decrease the specific force$F_o^{m(ox)}$, due to the power exponent$m\approx 2-7$. This, in turn, would rapidly decrease the decay constant ϵ_c which would lead to a more intensive stress relaxation process. As such, although the mutual amplitude,$\acute{F}_o$, is increased, however, after a "critical" (short) relaxation time, t_{cr}, the resultant mutual stress is further reduced, compared to the behaviours of the initial substrate thickness. This is schematically described in Fig (6).

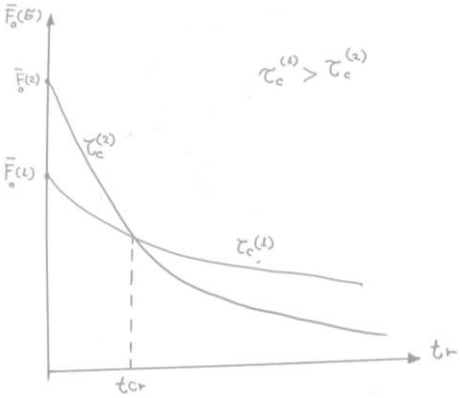

Fig (6) *Thickness reduction-induced mutual stress relaxation behavior of system Ni-surface layer/oxide substrate (1) initial thickness, (2) reduced thickness.*

Consequently, the so reduced thermal stresses in the denominator of Eq (5), may potentially act as weakened substrate constraints imposed on the Ni – surface layer which, under the influence of temperature, may more easily relax. This in turn would alter substantially the thermal strains measured in this (sensor) layer and consequently the data obtained for the required parameters.

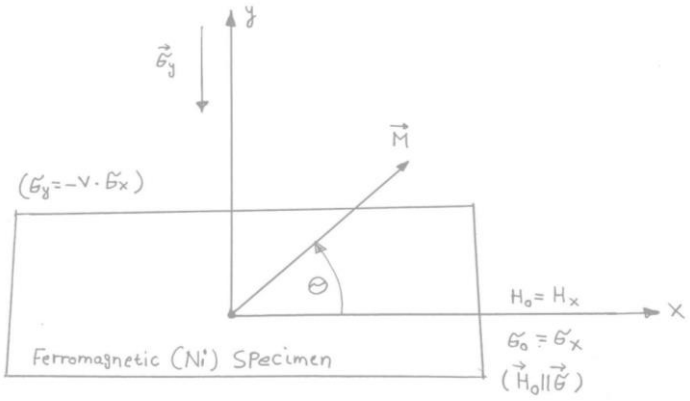

Fig (7) *X-axis ≡ direction of applied stress (6_o) and magnetic field (Ho). $\vec{M}$ is the magnetization vector rotating towards y-axis of thermodynamic equilibrium.*

Appendix III

MBE – principle

As mentioned in the text, the MBE presents the micromagnetic phenomenon – based macrosopical response of a magnetic material to applied stresses (strains) and/or to residual internal stresses. In this sense, the use of MBE becomes very important since the stresses in this material can reasonably be evaluated and at the same time the stress – induced microstructural changes can also be investigated. For this reason some basic features of MBE – principle are presented in the following. As described in the sketch of Fig (7) a magnetic specimen is subjected to a uniaxial tensile stress = 6_o with $6_o = 6_x$ = x-axis stress and $H_o = H_x$ = applied magnetizing field in direction of x – axis. Thereafter, it is known that $6_x = E\varepsilon_x$ and $\varepsilon_y = -V\varepsilon_x$ and also $6_y = E\varepsilon_y = -EV\varepsilon_x = -V6_x$ with V= Poisson ratio of material, with$0 < V \leq 0.5$.

It is also known that [18]:

$$E_p = \mp\frac{3}{2}\cdot\lambda_s\cdot 6\cdot cos^2 \quad \text{(III-a)}$$

for $\lambda_s > 0, (\lambda_s < 0)$

Here, E_p is the potential energy of a magnetic domain determined by the magnetization vector $\vec{M}$ in function of magnetostrictive saturation constant,λ_s, applied stress 6 and angle of orientation θ respective to the x-axis. It is mentioned that $\lambda_s >$ for Fe and $\lambda_s < 0$ for Ni. In the case of Ni ($\lambda_s < 0$) it can be shown:

$E_p = E_{max} = \frac{3}{2}\lambda\ \ 6$, for $\theta = 0°$ (III-b)

$E_p = E_{min} = 0$, for $\theta = 90°$ (III-c)

This means that for $\theta = 90°$ the magnetization vector $\vec{M}$ has rotated toward the y – axis which now becomes a stress – induced anisotropy axis of magnetization equilibrium, $M = M_y$. In this way, due to$6_y = -V6_o$, this axis is a compression stress one.

In other words, with increasing applied stress the magnetization vector tends to rotate towards the equilibrium y-axis by a simultaneous gradually decrease in the MBE-signal measured along x-axis. This fact could explain the behavior of the obtained MC of Fig (4), where the MBE-signal, $\acute{B}_t$, of Nickel decreases rapidly with applied stress. By the way, these statements should be able to demonstrate the wrong explanations given in [26] concerning the observed increasing rate of decrease in the MBE-signal after annealing of Ni, measured along the direction of increasing applied stress.

Correctly, this behavior should rather be attributed to a combined effect of an annealing-aided reduction of the number of pinning sites and in their pinning potential energy, fact which lead to more easy-free and hence rapid rotation of magnetization vector towards the compression y-axis of thermodynamic equilibrium, giving so a rapid reduction in ME-signal measured in the direction of x-axis of applied stress.

Appendix IV

A given stress-strain curve can be approximated by a power-hardening-type expression [13]:

$$6 = H\cdot\varepsilon_p^n \quad \text{(IV-a)}$$

which should be applied to the plastic strain region. Here, 0<n<1, is the strain hardening exponent and H the strength coefficient. Furthermore, it is:

plastic modulus=$\tan\beta=\frac{6}{\varepsilon_p} = H\cdot\frac{\varepsilon_p^n}{\varepsilon_p} = H\cdot\varepsilon_p^{n-1}$ (IV-b)

and $\varepsilon_p = \varepsilon_{th} = \Delta\propto(T)\cdot\Delta T$ (IV-c)

Thereafter, results that:

$$f(T) = tan_\beta = H\big(\Delta\propto(T)\big)^{n-1}\cdot T^{n-1} \quad \text{(IV-d)}$$

Now, during a cooling sequence from T_2 to T_1, one can obtain the following overall-average thermoplastic modulus function:

$$tan\acute{}_{\beta} = \int_{T_1}^{T_2} f(T)dT/\Delta T = H \cdot \int_{T_1}^{T_2} [\Delta\propto(T)]^{n-1} dT/\Delta T$$
(IV-e)

with $T_2 \gg T_1$ and $\Delta T = T_2 - T_1$ and$\Delta\propto=\propto - \propto_s \cong \propto \cong \propto_o \cdot (1 + b \cdot T)$. Thus, one may approximate as follows:

$(\Delta\propto)^{n-1} \cong \propto^{n-1} \cong \propto_o^{n-1} [1 + (n-1) \cdot b \cdot T]$ with $T_1 \leq T \leq T_2$ and $b \cdot T < 1$

Thereafter, equation (IV-e) becomes:

$$tan\acute{}_{\beta} \cong \acute{f}(T) = c_1 \cdot \int_{T_1}^{T_2} [1 + c_2 \cdot T] \cdot T^{n-1} \, dT/\Delta T$$
(IV-f)

Now, one can further approximate$aparabolicbehaviourofstress - straincurvewithn \cong 1/2$, within the plastic strain interval,$\varepsilon_y \leq \varepsilon \leq 6\%$, and consequently after some manipulations and a closed form integration procedure one can get:

$$tan\acute{}_{\beta} = \acute{f}(T) \cong T_2^{1/2} (c_3 - c_4 \cdot T_2)/\Delta T \cong$$
(IV-g)

with c_3/c_4 of the order of 10^4. We assume T_1= constant terminal cooling temperature and T_2= variable initial cooling temperature. In this may one can easily demonstrate that for an increasing (decreasing) thermal cooling range, the overall-average thermoplastic modulus should decrease (increase) causing so, potentially, an effective thermoplastic softening (hardening) effect in the Ni-material. It is mentioned hat in the above modelling approach creep-stress relaxation phenomena have been for simplicity neglected.

Table 1

Overall – average CTE, $\Delta T \cong 1400$℃	
$\acute{\propto}(\Delta T) \times 10^{-6}/$℃	$\acute{\propto}(\Delta T) \times 10^{-6}/$℃
Present measuring evaluation	Empirical evaluation
$\acute{\propto} \cong 17.9$	$\acute{\propto} \cong 16.8$ (24)
$\acute{\propto}_{Ti} \cong 13.8$	(22) $\acute{\propto}_{Ti} \cong 12.5$ (*)
$\acute{\propto}_{TiO_2} \cong 10.2$	(27) $\acute{\propto}_{TiO_2} \cong 9.0$ (*)
$\acute{\propto}_{Mn_3O_4} \cong 9.9$	$\acute{\propto}_{Mn_3O_4} \cong 8.9$ (17)
$\acute{\propto}_{MgO} \cong 11.6$	(23) $\acute{\propto}_{MgO} \cong 13.1$ (*)
By the data of cited reference (-)	

Table 1 – A

Partially – overall CTE, $\Delta T_1 \cong (1450 - 700)$℃,	
$\acute{\propto}(\Delta T) \times 10^{-6}/$℃	$\acute{\propto}(\Delta T) \times 10^{-6}/$℃
Present measuring evaluation	Empirical evaluation
$\acute{\propto}^{(1)} = 20.1$	$\acute{\propto}^{(1)} = 19.3$
$\acute{\propto}^{(2)} = 14.7$	$\acute{\propto}^{(2)} = 14.1$

Table 2

Instantaneous CTE at 'T'		
$\propto(\Delta T)\times 10^{-6}/°C$	$\propto(\Delta T)\times 10^{-6}/°C$	
Present evaluation	Empirical evaluation	
$\propto\ (1400°C)=21.8$	$\propto\ (1400°C)=20.1$	(24)
$\propto_{Ti}(600°C)=13.3$	$\propto_{Ti}(600°C)=12$	(22)
$\propto_{MgO}(1000°C)=15.86$	$\propto_{MgO}(1000°C)=14$	(23)
$\propto\ (700°C)=16.5$	$\propto\ (700°C)=15.4$	(24)
By data given in cited reference (-)		

Table 3

$(\Delta T\cong 1450-T_R)$ Overall – average thermoelastic moduli	
Present measuring evaluation	Empirical evaluation (*)
$\acute{E}_{TiO_2}(\Delta T)\cong 191GPa$	$\acute{E}_{TiO_2}(\Delta T)\cong 208GPa$
$\acute{E}_{Mn_3O_4}(\Delta T)=119GPa$	$\acute{E}_{Mn_3O_4}\cong 108GPa$

Remarks to Table 3: (*) performed by formula (13) given in the text and using the following data: $E_o(Mn_3O_4)=130MPa$ and $E_o(TiO_2)=230MPa$ taken from reference (26) and (27) respectively. $T_m(TiO_2)=1830°C$, $T_m(Mn_3O_4)=1705°C$ taken from reference (4) (T_m= melting point).

Table 4

Modulus [GPa]	δ-parameter $(E_o/\acute{E}_{op})-1$	Strain [%] $(\varepsilon_o=\varepsilon_R)$
$E_o=190$	1	0.0
$\acute{E}_{op}=25$	$13x10^{-2}$	0.5
$\acute{E}_{op}=13$	$7x10^{-2}$	1.0
$\acute{E}_{op}=11$	$6x10^{-2}$	2.0
$\acute{E}_{op}=8$	$4x10^{-2}$	2.8

MBE-measuring probe	
Reference surface (top) Nickel layer $(\propto_o, E_o)$	$t_o=t_{Ni}$
Substrate layer (1) $(\propto_1, E_1)$	t_{s1}

Substrate layer (2) $(\propto_2, E_2)$	t_{s2}
Substrate layer (i) $(\propto_i, E_i)$	t_{si}
Substrate layer (n) $(\propto_n, E_n)$	t_{sn}

Fig. (1) *Sketch of a thermally expanding-contracting multisubstrate-structured material system of a specimen characterized by* $(\propto_i, E_i)$ *and thickness* t_{si}*. MBE-measuring magnetic probe attached to the specimen.*